ANNALS OF WEST UNIVERSITY OF TIMISOARA PHYSICS
Vol. LXIV, 2022

DOI: 10.2478/awutp-2022-0001

A COMPARATIVE STUDY OF UN-DOPED ZnO AND In DOPING ZnO THIN FILMS WITH VARIOUS CONCENTRATIONS, SUBJECTED TO APPROPRIATE UHV TREATMENT AND CHARACTERIZED BY SENSITIVE SPECTROSCOPY TECHNIQUES XPS, AES, REELS AND PL

Kadda Benmohktar Bensassi[1,2], Edhawya Hameurlaine[1*], M'hamed Guezzoul[1], M'hammed Bouslama[1], Abdellah Ouerdane[1,3], Abdelkader Belaidi[4], Amira Derri[1], Mahmoud Bedrouni[1], Abdelhak Baizid[1], Mahfoud Abdelkrim[1], Bachir Kharoubi[5]

[1]*Laboratory of materials (LABMAT), National Polytechnique School (ENP) of Oran, BP1523 Oran Mnaouar, Oran, Algeria*
[2]*Laboratory of Electron Microscopy and Materials Science, University of Science andTechnology Mohamed Boudiaf of Oran, Algeria*
[3]*University of Djilali Bounaama-Khemis Méliana, Ain Defla, Algeria*
[4]*Laboratory of Automatics and Systems Analysis (L.A.A.S), National Polytechnique School (ENP) of Oran, BP 1523 Oran Mnaouar, Oran, Algeria*
[5]*Research Laboratory of Industrial Technology, Faculty of Applied Sciences, Universityof Tiaret, Algeria.*
[*]*Corresponding author:* ***hameurlainedhawya27@gmail.com***

Article Info

Received: 01.11.2021
Accepted: 22.02.2022

Keywords:
UHV physical treatment; AES; XPS; PL; REELS; chemical composition; physical structure

Abstract

In this study, we use complementary and sensitive experimental techniques XPS (X-rays Photoelectron Spectroscopy), AES (Auger Electron Spectroscopy, REELS (Reflection Electron Energy-Loss Spectroscopy) and PL (photoluminescence) to investigate and compare the chemical, structure, electronic and optical properties of Un-doped ZnO (UZO) and Indium-doped ZnO (IZO) (4% In; 6% In) thin films. Spray method is used for the growth of these thin films on Si substrate. A treatment process UHV (Ultra-High -Vacuum: Ar+ sputtering followed by checked successive heating until 650°C) is performed. XPS and AES results allow to confirm the clean state of samples and the incorporation of indium into the ZnO matrix to form chemical species of (In-O-Zn) type. The recorded REELS spectra at different primary energies and the PL measurements justify that the UHV treatment plays an important role to improve the physical structure of IZO (6% In).

1. Introduction

Zinc oxide (ZnO) is a semiconductor with direct wide band gap (3.37eV) and a large exciton energy of 60 meV at room temperature [1]. ZnO is of excellent electronic and optical proprieties applied as solar cell [2], water splitting [3], varisitors [4], sensor or nano-generators [5], super capacitors [6], light emitting diodes [7] etc.

It was reported that Un-doped ZnO thin films are not stable especially at high temperatures. So, the ZnO doping is susceptible to reduce this disadvantage [8]; it is the most efficient ways to increase its functionality as TCO [9].

Among the III group elements, the indium is considered well appropriate for the ZnO doping [10]. It allows to increase the carrier concentration of ZnO [11], improve the electrical conductivity [12] and useful for applications in many devices as flat panel displays [13], transparent electrodes [14], solar cells [15] and light-emitting diodes (LEDs) [16]. The growth process of ZnO thin film might be achieved according to chemical vapor deposition (CVD) [17], RF magnetron sputtering [18], thermal evaporation [19] and spray pyrolysis [20]. We adopt the last technique (spray pyrolysis) for the preparation of Un-doped ZnO (UZO) and In-doped ZnO (4% In, 6% In) on Si substrate because of its great advantages (low cost, simplicity, ability to deposit thin films on broad areas, non-vacuum required and high deposition rate. Moreover, the performance of technological applications depends on the physical structure and the chemical composition of ZnO films. The surface of compound must be clean. Different treatments for cleaning ZnO surface are reported in literature: argon ion sputtering [21], UV-ozone treatment [22], thermal annealing [23] and oxygen plasma treatment [24]. We adopt a checked UHV (Ultra High Vacuum) treatment by argon ion sputtering followed by successive heating at different temperatures. Different reported results showed the ZnO doping by indium at various concentrations: low (0-5 at%) [25], moderate (5-10at%) and high (> 10at%) [26].

The aim of this work is to study the influence of UHV treatment on the indium doping of ZnO at low (4 at %) and moderate (6 at%) concentration of point of view chemical, structural and optical properties. We use sensitive and complementary analysis techniques such as XPS (X ray photoelectron spectroscopy), AES (Auger Electron Spectroscopy), REELS (Reflection Electron Energy Loss Spectroscopy) and PL (Photoluminescence). The XPS and AES are powerful analysis techniques to display the chemical composition of thin films UZO and IZO (4% In, 6% In). The REELS is an analysis technique complementary to XPS and AES and able to display the electron distribution in the valence band of compounds. We use the PL technique very useful for studying the electron states in the gap. We establish the complementarity link between the experimental techniques XPS; AES; Pl and REELS.

2. Experimental

2. 1. Preparation of UZO and IZO thin films

The Chemical Ultrasonic Spray Pyrolysis technique is used to prepare the un-doped (UZO) and Indium doped ZnO (4% In, 6% In) thin films deposited on Si substrates.

For UZO, we dissolve the hydrated zinc acetate (Zn $(CH_3COO)_2.2H_2O$) into 100 ml of methanol with the molar concentration of 0.3 mol/l. For IZO, we use hydrated indium chloride ($InCl_3$. $2H_2O$) as dopant. We maintain the respective molar ratio concentration (In/[In+Zn]) in the precursor solution at 4% and 6%. The solutions are stirred at 400°C during 1 hour to ensure its chemical homogeneity.

2. 2. Characterization details and UHV physical treatment

The undoped ZnO (UZO) and Indium doped ZnO (IZO) samples are characterized by XPS; AES and REELS in the analysis chamber where the pressure is of 2×10-10 mbar using Scienta Omicron Ultra High Vacuum (UHV) system involving an electron gun and X-Ray source. The UHV treatment is achieved in the preparation chamber including an Ion gun of cold cathode sputter ion source ISE 5. The argon gas is introduced through a leak valve to reach the pressure of 2.10-6 mbar. The energy and the current of the ion beam are 1.2 KeV and 3µA, respectively. The argon ion sputtering is achieved during 15 min to clean the surfaces. The samples are then submitted to heating process in the same conditions using a standard manipulator with PBN (Pyrolytic Boron Nitride) resistive heater as follow: (350°C during 20 min), (500°C during 20 min) and (650°C during 40 min).

2.2.1. X- Ray source

The X-Rays are obtained from DAR400 (Dual anode X-Ray) type source. The XPS spectra are recorded by using the monochromatic Mg-Kα excitation line (hν=1253.6eV) corresponding to anode voltage and emission current 15KV and 15mA, respectively with a power (P=225W).

The spectrometer is calibrated by using the photoelectron emission state Ag 3d5/2 at 368.2eV. The binding energies of XPS spectra are calibrated on the basis of signal C1s at 284.8eV [27].The concentrations (At%) of zinc, oxygen, carbon and indium of UZO and IZO are calculated through the Zn 2p3/2, O1s, C1s and In3d5/2 signals by CasaXPS. The relative sensitivity factors (RSF) of different elements are derived from Casa-XPS such as: (18 for Zn 2p3/2); (2.85 for O 1s); (1 for C1s) and (13.23 for In3d5/2).

2.2.2. AES and REELS (electron source)

The AES and REELS spectra are recorded using an electron gun SL1000 involving a LaB6 (Lanthanum Hexaboride) tip of high performance for providing an electron beam of constant energy 3500eV for AES and variable energy (100eV to 1000eV) for REELS. We use a hemispherical spectrometer (128 channels) of high resolution and transmission with a pass energy of 50eV.

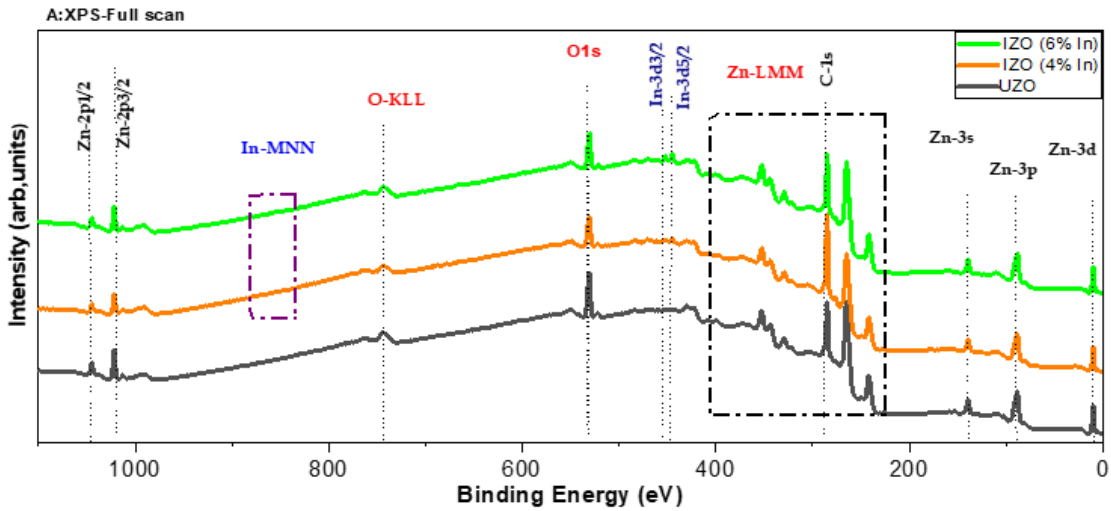
2.2.3. Photoluminescence source

The room temperature photoluminescence (PL) is performed using the spectrometer HORIBA iHR-550 equipped with CCD detector (400-1000 nm) and InGaAs detector (800-1600 nm). The He-Cd laser of wavelength 325nm (UV) and power 30mW is used as excitation source.

3. Results and Discussion

3. 1. X-Ray spectra of UZO and IZO (4%In; 6% In) at the initial state (as prepared samples)

XPS (X ray photoelectron spectroscopy) is a powerful technique allowing us to identify the chemical composition of UZO and IZO thin films grown on the Si substrate**.** Fig.1A shows the XPS full scan of Un-doped ZnO (UZO) and Indium doped ZnO (IZO) at 4% In and 6% In at the initial state (as prepared sample). The signals of elements: Zn, C and O do appear (except the In signal which is barely visible on Fig. 1A: it is less resolved because of the influence of the contamination layer and its weak concentration).



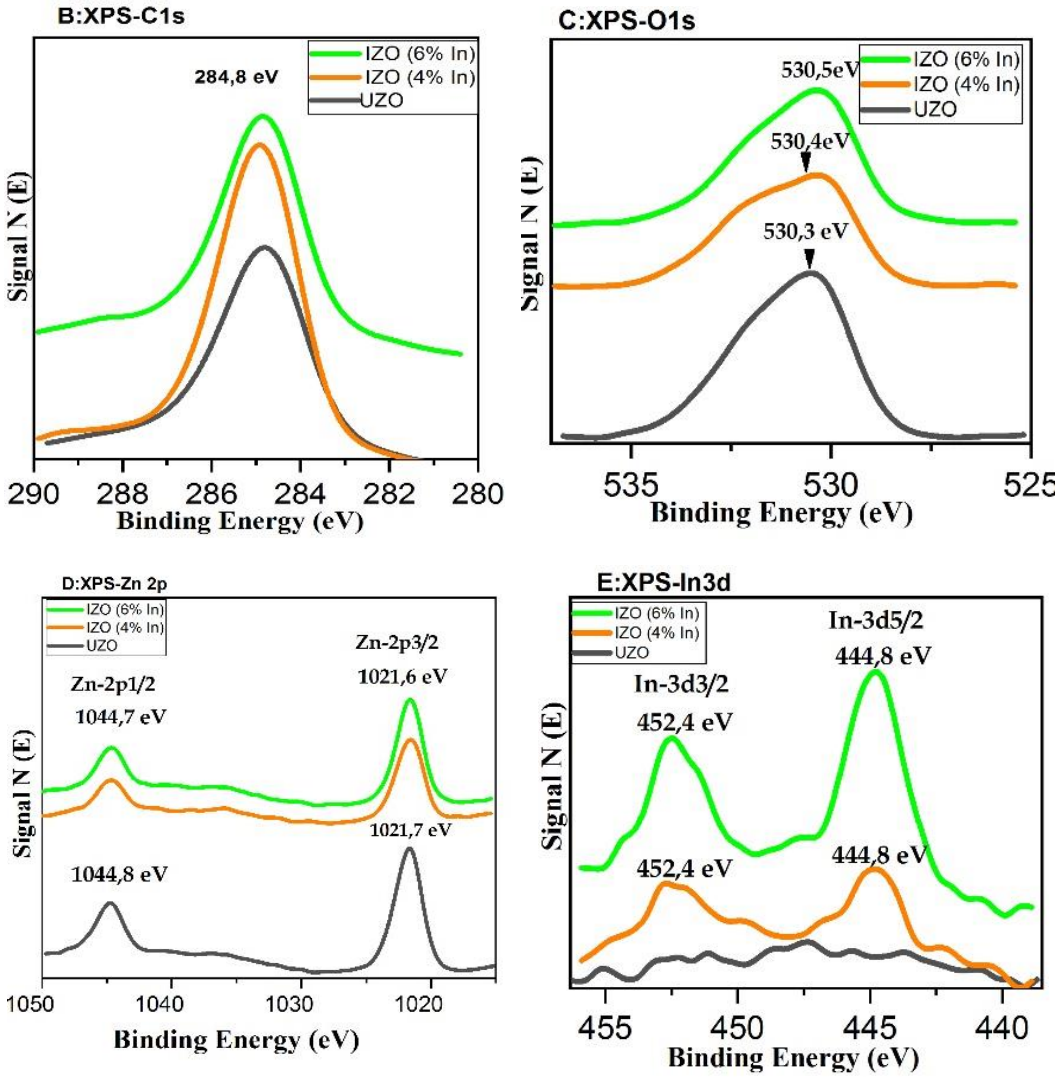


Figure1. A: XPS spectra of UZO and IZO (4% In, 6% In) at the contaminated state. B; C; D and E correspond to amplificated signals C 1s, O 1s; (Zn2p3/2; Zn2p1/2) and (In3d5/2; In3d3/2)

As shown in Fig.1B, the carbon signal C1s of IZO (6%In) is more important than the IZO (4% In) one. This means the IZO (6% In) is more contaminated by the carbon impurity. Fig.1C displays the O1s signal with a binding energy at (530.3eV for UZO); (530.4 eV for IZO (4% In)) and (530.5 eV for 6% IZO (6% In)). The XPS spectra of zinc are shown Zn 2p in Fig.1D. The electron states $Zn2p_{3/2}$ and $Zn2p_{1/2}$ are located at (1021.7 eV; 1044.8eV) for UZO and (1021.6eV; 1044.7eV) for both IZO (4% In and 6% In). The binding energies are different from the UZO ones but similar for the IZO samples because their surfaces are not clean. The incorporation of indium into the ZnO matrix induces the change of the binding energy of electron states of zinc. So, a chemical reactivity is susceptible to occur between zinc, indium and oxygen. We will discuss this point clearly through the XPS results of clean UZO and IZO. The XPS spectra related to indium are shown in Fig.1E. The peaks related to electron states (In3d5/2; In3d3/2) of IZO (6%In) are well resolved appearing at the binding energy (444.8 eV;

452.4eV). But; These peaks are less resolved for IZO 4% In). The chemical composition (At%) of UZO and IZO atthe contamination state (as prepared samples) is given in table 1 on the basis of XPS spectra.

We clearly see that the carbon proportion is of (52.77% for UZO, (61.43% and 63.69%) for IZO (4% In and 6% In), respectively). Thus, the carbon contamination layer has an effect on signals of Zn, O1s and In3d.We notice that UZO is less affected by the contamination layer than IZO. However, IZO (6% In) is more contaminated by the carbon than IZO (4% In). The oxygen proportion (At%) of O1s decreases with the increasing of Indium doping.

Table 1. The chemical composition (At % of different elements of UZO and IZO at the initial state (as prepared samples)

		Elements (At %)			
	Sample	Zn	O1s	C	In
UZO	Untreated	12.21	34.92	52.87	/
IZO 4 at %	Untreated	12.33	26.05	61.45	0.17
IZO 6 at %	Untreated	11.98	24.20	63.19	0.63

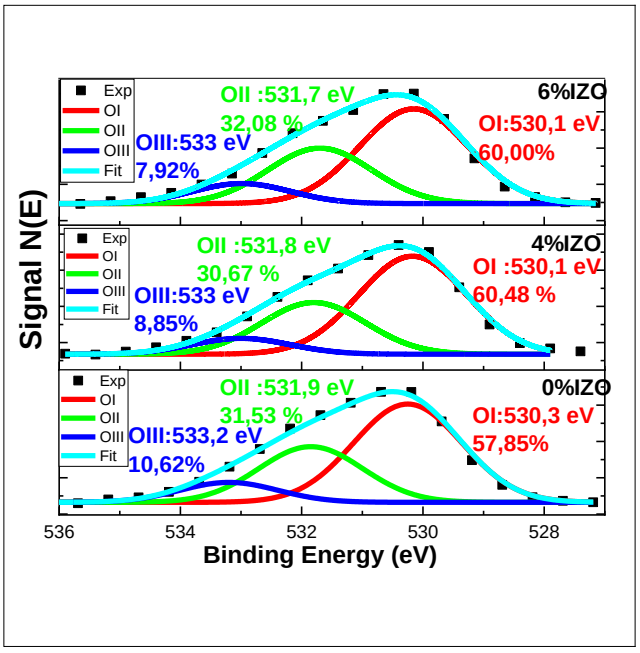


Figure 2. O1s Gaussian deconvolution of UZOand IZO (4% In, 6% In) at the contaminated state (as prepared samples

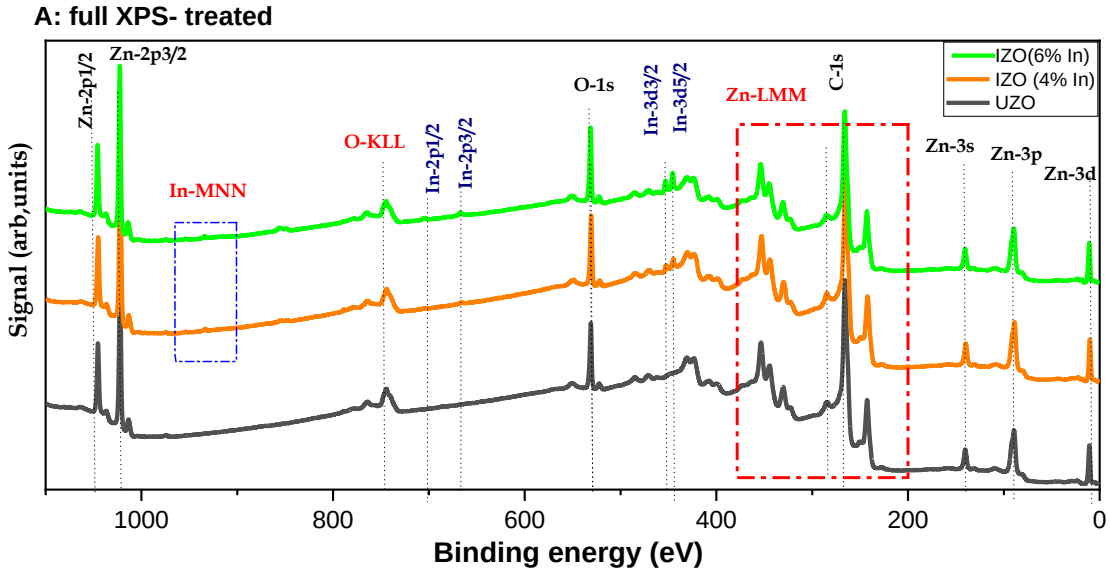
We discuss the O1s shape on the basis of Gaussian deconvolution shown in Fig. 2. The O1s spectrum is asymmetric. The Gaussian deconvolution of O1s shows three peaks. For UZO, the first peak OI located at 530.3eV is attributed to O-Zn bonds. The second peak OII located at 531.9 eV is attributed to oxygen-deficient regions within the matrix of ZnO. The last peak

OIII located at 533.2eV is related to impurity species as hydroxides and/or carbon oxides adsorbed on the surface in agreement with reported results [28].

For IZO, the O1s is also asymmetric, involving three peaks. The two peaks OI andOII appear at (530.1 eV; 531.8 eV) for IZO (4%In) and (530.1eV; 531.7 eV) for IZO (6% In). They are related to the oxygen bounded as (Zn-O and O-In) and oxygen vacancies, respectively. They are broader than the UZO ones. The third peak O_{III} located at 533 eV is related to impurity species (hydroxides and / or carbon oxides adsorbed onthe surface. We notice that the OI proportion (57.85 %) for UZO is lower than IZO one. However, OII and OIII proportions for IZO (4% In) and IZO (6% In) are of (30.67%; 8.85%) and (32.08%;7.92%), respectively. They are lower than those related to UZO (31.53%; 10.62%). We deduce that the indium doping is susceptible to create oxygen-deficiency.

3. 2. X –Ray photoemission spectroscopy of UZO compared to IZO after UHV treatment (clean surfaces)

Figure 3-A represents the XPS full spectrum of UZO and IZO (4% In, 6% In) thin films after UHV physical treatment (Ar^+ ions sputtering followed by described heating previously).



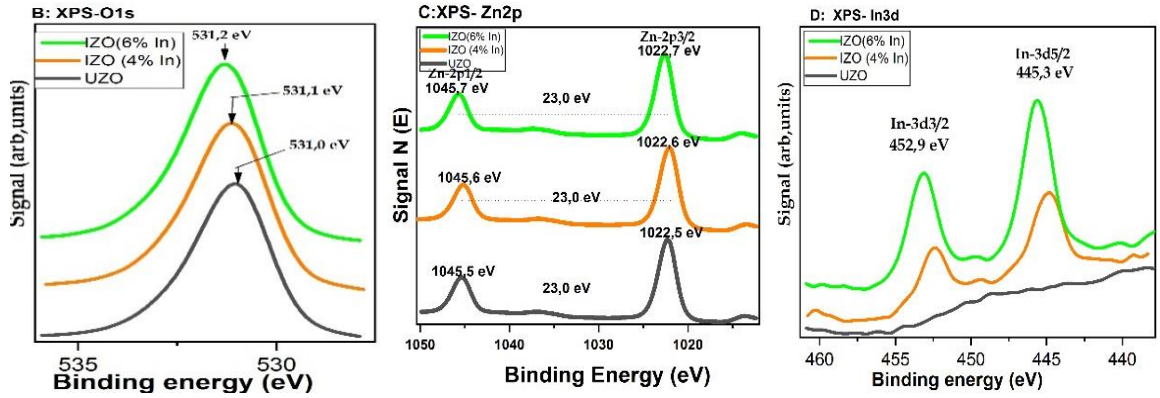


Figure 3. A: XPS spectra of: UZO and IZO (4% In ,6% In) after UHV physical treatment.
B, C, D: Amplificated O 1s, (Zn2p3/2; Zn2p ½) and (In3d5/2; In3d3/2) signals

The signals of C1s and C KLL vanish significantly and there is an enhancement of signals related to zinc, oxygen and indium. This means that the UHV physical treatment allowed to remove the contamination layer of carbon. The surfaces become clean. Fig. 3B shows the increase of the intensity of O1s with displacement towards higher energy (ΔE=0.8 eV for UZO, ΔE=0.6eV for IZO (4% In) and ΔE=0.5eV for IZO (6% In).

Besides, the XPS spectrum shown in Fig. 3C involves a double peak corresponding to electron states Zn 2p1/2 and Zn2p3/2, with a spin-orbit splitting of 23.0 eV for UZO and IZO in agreement with reported results [29]. However, the electron states Zn2p1/2 and Zn3/2 shift slightly to higher binding energy for IZO in comparison with UZO.

The electronegativity values of In and Zn are (χ =1.78) and (χ=1.65) respectively [30]. They advantage chemical bonds to occur between oxygen, indium and zinc. We clarify this point through the shape of XPS and AES spectra.

Fig. 3D shows the core level of In 3d of IZO (4% In and 6% In) of Spin-orbit coupling states 7.6eV [31]. We discuss particularly the electron states 3d5/2 and 3d3/2. They are of significant intensities and well resolved in comparison with the IZO (4% In) ones. These two peaks are of binding energy (445.3eV, 452.9 eV). We notice that the electron states In3d5/2 and In3d3/2 related to indium oxide (In2O3) are of binding energies (444.0eV and 451.6eV) as reported in literature [32]. The electron states In3d5/2 and In3d3/2 related to indium metal are of binding energy (451.1eV and 443.7eV) [33]. We deduce that the incorporation of indium into ZnO matrix does not lead to form In metal or In2O3. Furthermore, the achieved heating temperature of samples at 650°C is very higher than the melting point of indium metal (123°C). Such a temperature does not advantage the formation of indium metal into the ZnO matrix. On the basis of these results, we suggest that the binding energy of 3d5/2 and 3d3/2 of indium in Fig. 3D correspond to electron states related to chemical species of In-O-Zn type in agreement

with reported results [34]. The calculation of (At% composition) of different elements of UZO and IZO (4% In) and IZO (6% In) are shown in table 2.

Table 2: chemical composition of UZO and IZO (after UHV treatment).

		Elements (At %)			
	Sample	Zn	O1s	C	In
UZO	Treated	36.12	57.28	6.6	/
IZO 4 at %	Treated	35.82	58.18	2.15	3.85
IZO 6 at %	Treated	35.42	58.20	0.83	5.55

We see that the zinc proportion (At%) reduces after the UHV treatment. However, (At%) of indium increases. This means a partial desorption of zinc atoms. The UHV treatment allows a convenient incorporation of indium atoms into ZnO matrix to occupy the sites due to zinc vacancies [35]. We show in Fig. 4 the Gaussian deconvolution of asymmetric O1s peaks of UZO and IZO (4% In; 6% In). The Gaussian deconvolution allows the appearance of two peaks OI and OII. The OI peak is ascribed to chemical bonds (oxygen- zinc) for UZO) and (oxygen-zinc-indium) for IZO. The peak OII is related to oxygen vacancies as discussed previously. The contribution of OI is of 22.65% for IZO (6% In). It is the most reduced in comparison with UZO and IZO (4% In). The checked UHV treatment and the indium choice of the indium concentration (6% In) are very appropriate to ensure a homogenous structure of IZO (6% In) lattice. So, chemical bonds between oxygen; zinc and indium occur and the oxygen vacancies reduce.

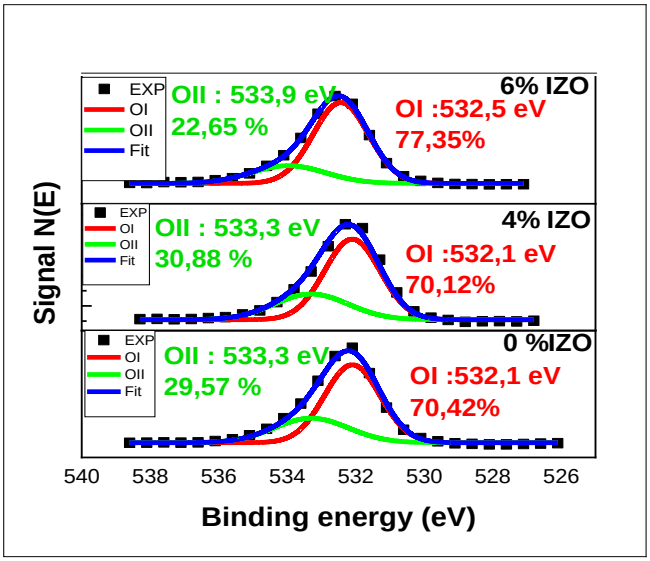
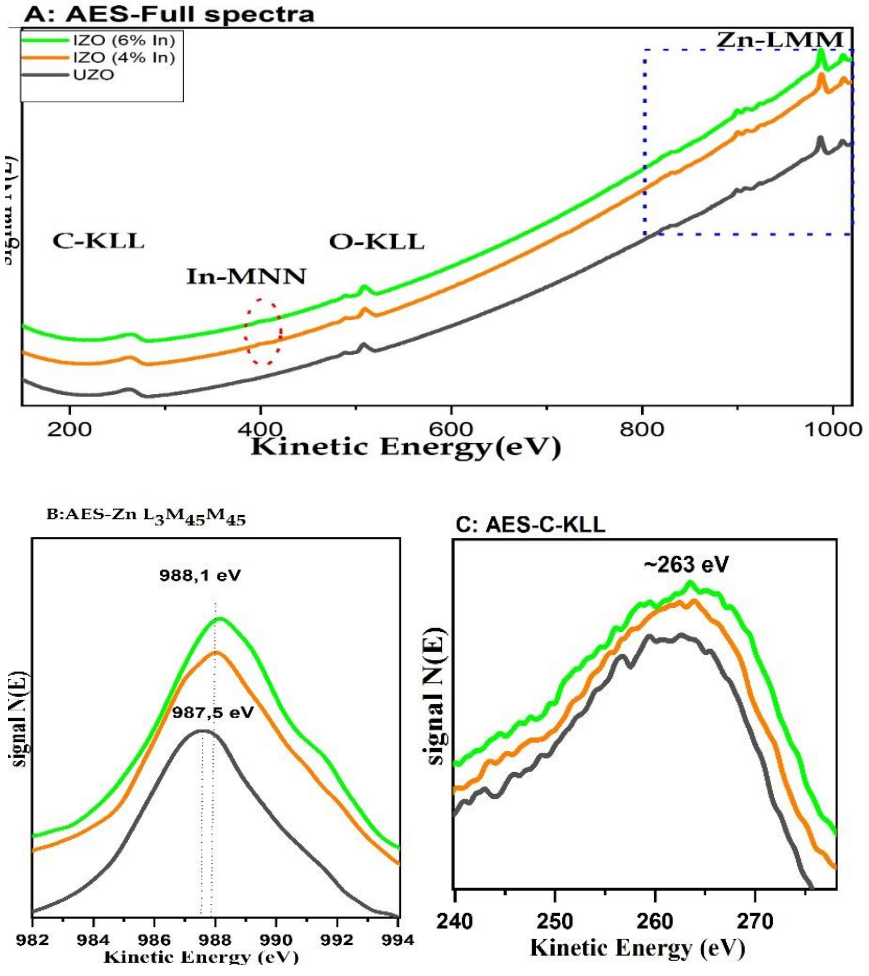


Figure 4. Gaussian deconvolution of O1s of UZO and IZO (4% In and 6% In) after UHV treatment

3. 3. AES results of UZO and IZO before UHV treatment

AES is an analysis technique complementary to XPS. The AES technique is of high sensitivity to analyze the chemical environment of upper layers of thickness of about 50 Å of materials.

Fig. 5A presents the AES full scan (at the initial state) of UZO and IZO. The Auger transitions are related to zinc, oxygen and carbon (Zn- LMM; O-KLL and C-KLL). For IZO; the transition In-MNN is barely visible because of the influence of the carbon contamination layer and its weak concentration. We give in Fig. 5B the AES spectrum Zn- L3M45M45 of UZO and IZO. The kinetic energy of Zn L3M 45M45 of UZO is lower than the IZO one (shift of 0.6eV). It is also the case for the O-KLL signal (shift of same value 0.6eV; see Fig. 5D). This means that the indium incorporation into ZnO matrix induces a new atomic arrangement of zinc, oxygen and indium. The amplificated Auger signals C-KLL is shown in Fig. 5C. In AES, the Auger signal In-MNN appears with weak intensity and broad shape (less resolved; see Fig. 5E) in comparison with the XPS signal shown in Fig. 3D because the analyzed depth in XPS is more important (about 100Å). We deduce that the analyzed upper layers by AES (50Å) involve an important contamination layer of carbon.



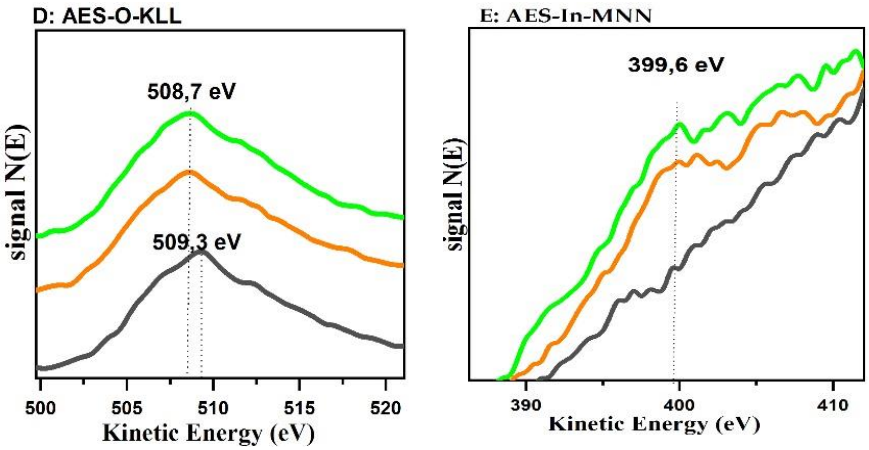


Figure 5. A -Full scan of AES spectra of UZO and IZO (4% In, 6% In) before UHV treatment (as prepared samples); B, C , D and E: amplificated Auger transitions Zn-$L_3M_{45}M_{45}$, C-KLL, OKLL and In-MNN

3. 4. AES spectra after UHV treatment

Fig. 6A displays the AES full scan of UZO and IZO (4% In and 6% In) after the UHV treatment. There is disappearance of C-KLL signal and enhancement Auger signals related to zinc, oxygen and indium. We show in Fig. 6B, C, D the amplificated Auger signals of these elements. The kinetic energy of Auger transition related to Zn-$L_3M_{45}M_{45}$ of IZO is lower than the UZO one. This means that the UHV treatment induces a better arrangement of zinc atoms in comparison with Fig. 5. The UHV treatment is of great interest to ensure a structural stability of IZO (6%In) particularly. This result is also justified by the lower kinetic energy of Auger electron related to the transition O-KLL of IZO (6% In) in comparison with the UZO and IZO (4% In) ones, as shown in Fig. 6C. The main peak related to the Auger electron transition In-M5N45N45 of indium is of kinetic energy 399.7eV as shown in Fig. 6E. Such an energy is different from the ones related to indium oxide (In2O3: 398.6eV) [36] and metal indium (In-In: 402.6eV) [37]. Thus, we deduce that the incorporated indium into the ZnO matrix is susceptible to form chemical bonds of In-O-Zn type in agreement with discussed results**.**

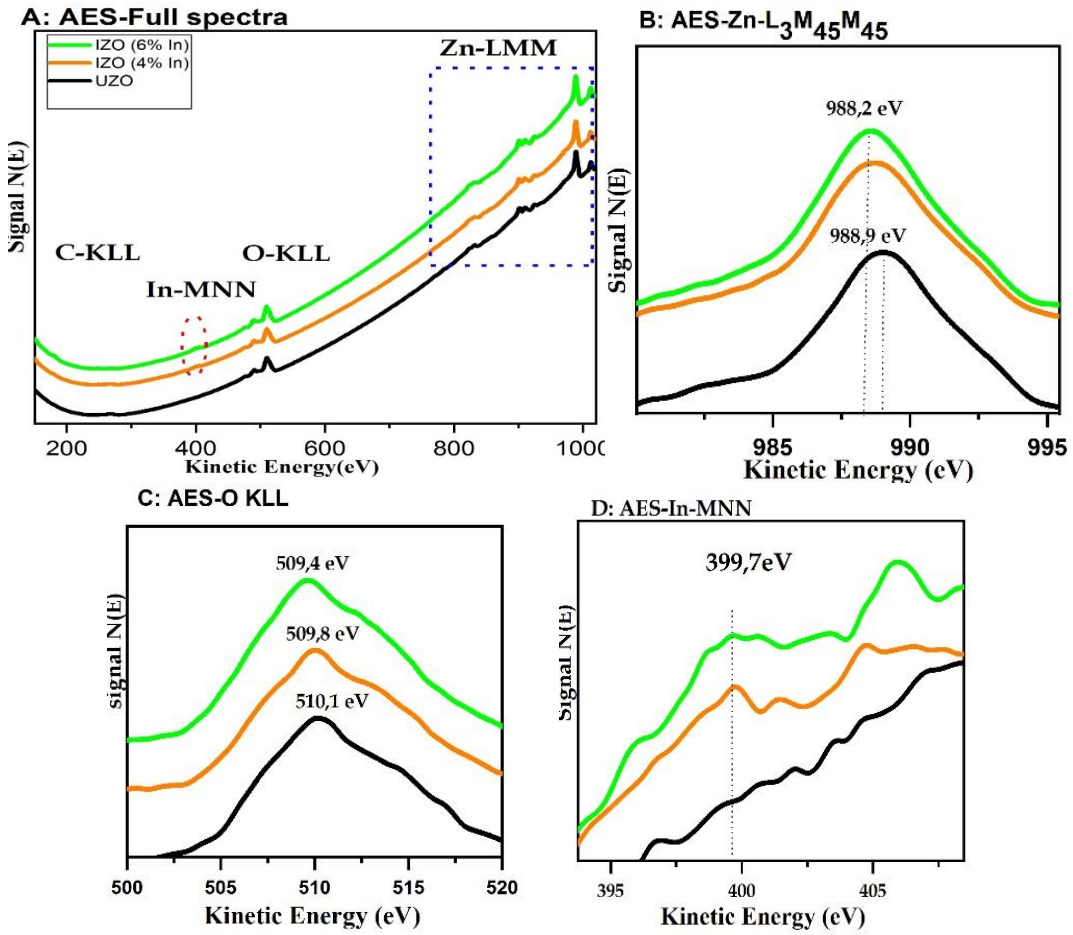


Figure 6. A: AES spectra (full scan) of UZO and IZO (4% In; 6% In) after UHV treatment B, C and D: Resolved Auger transitions of Zn L3M45M45, O KLL and In MNN

3. 5. PL (Photoluminescence) results

The Photoluminescence spectroscopy is a sensitive technique of great usefulness for displaying the electron states in the gap of semiconductor materials. A comparative study of UZO; IZO (4% In; 6% In) is performed by the photoluminescence measurements before and after the cleaning UHV treatment (described previously).

We notice that the band gap is of ZnO is of 3.34 eV by taking into account the exciton energy of 60 meV [38-39].

3.5.1. Photoluminescence PL Measurements before UHV treatment (as preparedsamples)

Fig.7 shows the recorded photoluminescence (PL) spectra of UZO and IZO (4% In; 6% In) at the initial state (as prepared samples). We discuss the photoluminescence results on the basis of energy diagram shown in Fig. 8.

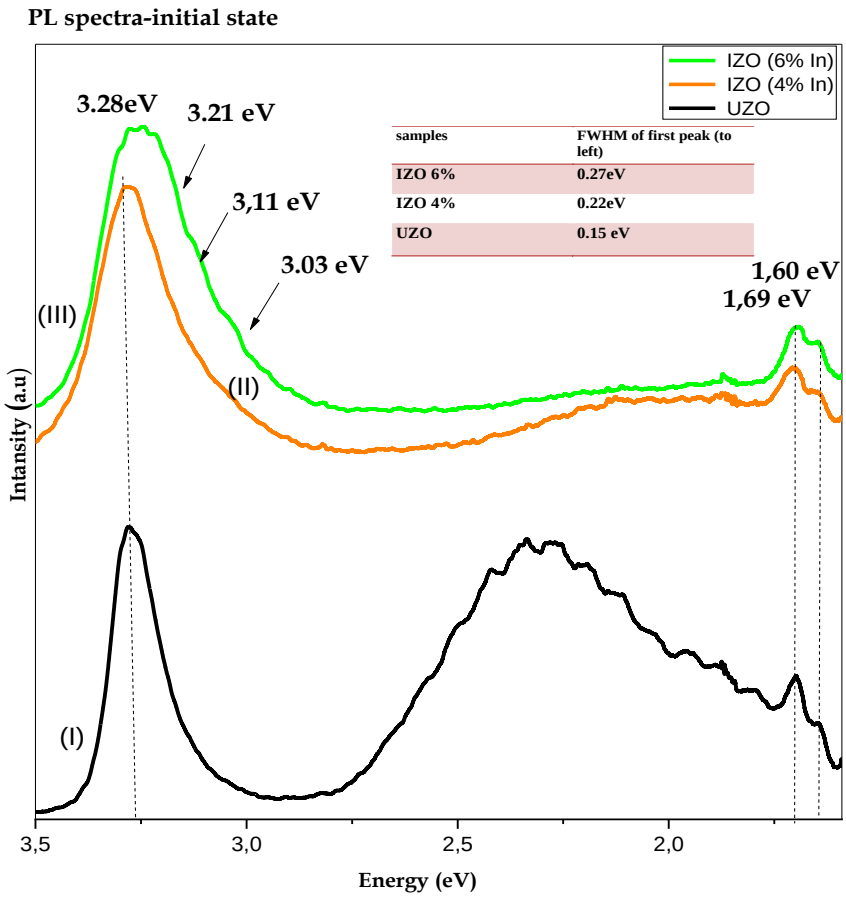


Figure 7. PL spectra with the FWHM values of first peak (to left) of UZO and IZO (4%In,6%In)

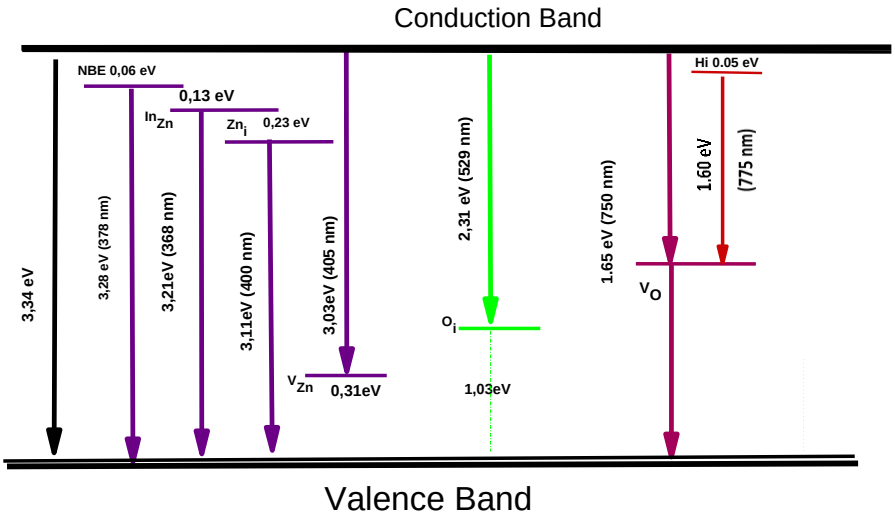


Figure 8. IZO band diagram with the approximate positions of defect levels and luminescence mechanisms as suggested by other authors: NBE (Near Band Energy) [40]; In_{Zn} (substituted zinc by indium)[42], Zn_i (zinc interstitial)[43], V_{Zn} (zinc vacancies)[44], Oi (interstitial oxygen) [41], Hi (interstitial hydrogen) [48], V_O (oxygen vacancies) [46-47]

For UZO; the PL spectrum I involves a first peak to left of high intensity at 3.28eV (378nm). The emission of 3.28eV concerns the electron transitions from the states near band

edge (NBE) of energy 0.06eV [40] under the bottom of the conduction band to the valence band maximum (VBM), as shown on the schematic energy diagram (see Fig. 8). Another type of emission does appear with abroad peak around E=2.31eV (536 nm) corresponding to green emission. It is due to electron transitions from the conduction band (CB) to the electron states related to oxygen interstitial (O_i) of energy level 1.03eV in agreement with other results [41] as indicated on the energy band diagram in Fig. 8. The PL spectra (II and III) shown in Fig. 7 are related to IZO (4% In; 6% In). In particular; the first peak of PL spectrum III is the broadest in comparison with the two other PL spectra (I and II) because of the higher indium concentration (6%) incorporated into the ZnO matrix. The size of indium atoms (0.080nm) is bigger than the zinc atoms one (0.074nm). Thus, the incorporation of indium into the ZnO matrix induces structural defects as zinc vacancies (V_{Zn}) and interstitial of zinc atoms (Zn_i) in agreement with the discussed results in the XPS and AES parts previously. The indium atoms are susceptible to restitute the zinc atoms to occupy the zinc vacancies to create electron states In_{Zn} of energy 0.13eV under the bottom of the conduction band. The electron states (V_{Zn}) are of energy 0.31eV above the valence band maximum (VBM). The electron states (Zni) are of energy 0.23eV under the bottom of the conduction band, as shown on the schematic band diagram (Fig. 8). We give in inset (Fig. 7) the values of FWHM of PL spectra (I; II and IIII). We notice that the PL (spectrum III) of IZO (6% In) involves shoulder peaks. The first located at 3.21 eV (386 nm) corresponds to electron transitions from In_{Zn} electron states to the valence band maximum (VBM)[42]. The second peak located at 3.11 eV (400 nm) is related to electron transition from interstitial zinc (Zni) to the valence band maximum (VBM) [43]. The third peak located at 3.03eV(410nm) corresponds to emissions from the bottom of the conduction band (CB) to zinc vacancies (V_{Zn}), in agreement with reported results [44]. The maximum of broad PL peak of UZO is at 2.31eV. It corresponds to electron transition from the bottom of the conduction band to electron states Oi (interstitial oxygen) located at 1.03eV above the valence band maximum (VBM) . That green emission (2.31 eV) disappears completely after the incorporation of indium into ZnO matrix. The In doping of ZnO allows to reduce the structural defects as interstitial oxygen (Oi) [45].

In addition, Fig.7 shows a Near IR luminescence appeared for all the samples (PL spectra I; II and III) at 1.69eV (750 nm) and 1.6 eV (775 nm). The emission at 1.69 eV is related to the electron recombination from the oxygen vacancy states (Vo) located in the middle of the bandgap) to the states just under the valence band maximum (VBM) in agreement with reported results [46-47].

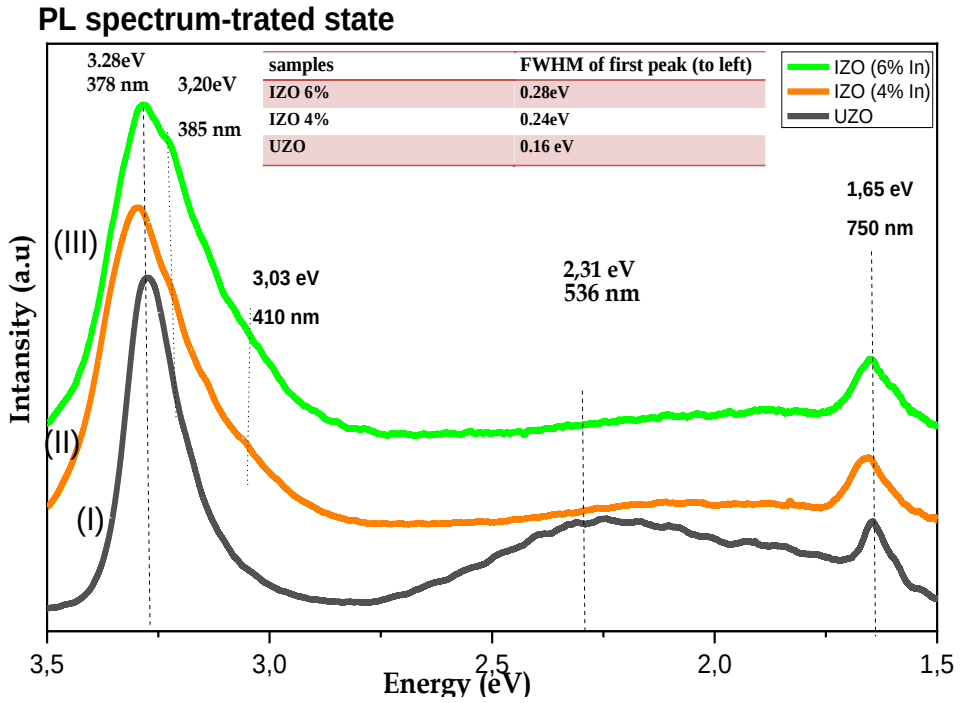
The other peak located at 1.6 eV (775 nm) corresponds to transitions from hydrogen

impurity Hi states located at 0.05 eV under the bottom of the conduction band (CB) to the oxygen vacancies (VO) [48] as indicated in the diagram (Fig. 8). So, the PL measurements are complementary to XPS and AES results previously described.

We then show the great advantage of PL measurements to explain the optical properties of materials.

3.5.2. Photoluminescence PL Measurements after UHV treatment

After the UHV treatment of samples; we show in Fig. 9 the recorded PL spectra of UZO (I) and IZO (4% In (II);6% In (III)). The main PL peak is well resolved and of high intensity in comparison with the PL spectra recorded in Fig. 7 (before the UHV treatment). We give the FWHM values for each spectrum in inset (Fig. 9). They increase significantly.



samples	FWHM of first peak (to left)
IZO 6%	0.28eV
IZO 4%	0.24eV
UZO	0.16 eV

Figure 9. PL spectra and the calculated the FWHM of UZO and IZO (at 4%,6%)

For UZO (spectrum I), the visible PL emission at 2.31 eV decreases significantly. The UHV treatment reduces states due to the structural defects related to interstitial oxygen (O_i).

For IZO (4% In, 6 % In) (see spectra I and II), the PL emission at 3.28 eV is of high intensity and well resolved and involving the shoulder peak at 3.21 eV as described in the section 3.5.1. The incorporated indium atoms into ZnO matrix contribute to substitute the desorbed zinc atoms to create the states In_{Zn} inducing the emission of 3.21eV related to electron transitions from In_{Zn} to valence band maximum (VBM).The emissions of energies 3.11eV and 3.03eV reduce significantly. They are barely visible. We deduce that the UHV treatment

allowed to eliminate the structural defects of zinc vacancies (V_{Zn}) and interstitial zinc (Zn_i). A convenient atomic arrangement occurs. The electron states due to zinc atoms located in interstitial sites (Zn_i) undergo a displacement toward convenient sites corresponding to NBE levels, justified by the enhancement of PL signal at 3.28 eV corresponding to electron transitions from NBE levels to VBM (Valence Band Maximum). Thus, In dopant plays an important role in the luminescence process . Besides, the green emission disappears completely [49].We notice that after the UHV treatment of samples, the peak related to the emission at 1.6 eV disappears completely for all the samples. This means that the hydrogen impurity (Hi) was removed by the UHV treatment.

3. 6. REELS results of UZO and IZO before and after UHV treatment

Reflection Electron Energy-Loss Spectroscopy (REELS) is a powerful analysis technique of materials of point of view chemical composition and electronic structure of high surface sensitivity [50]. We give in Fig. 10 the recorded REELS spectra at low and high primary energy (Ep=500eV and Ep=1000eV) before and after UHV treatment. Before the UHV treatment; the recorded REELS spectra in Fig10 (A; B) correspond to the contaminated state of the surface by carbon; hydroxides and carbon oxide). The peak corresponding to plasmons is located at 20eV. The peak appearing near the elastic peak at 4.8eV corresponds to interband transitions related to adsorbed oxygen among the impurity species.

After the UHV treatment; as shown in Fig.10 (C, D) the REELS spectra are more resolved than those recorded at the initial state (Fig.10 A, B). The REELS spectra involve main peak due to plasmons (surface and bulk) located at 18.9eV for UZO [51] and 18.5 eV for IZO (4% In; 6% In) [52]. There is a shift of 0.4 eV due to the indium incorporation into the ZnO matrix. The recorded REELS spectra at high primary energy Ep=1000eV show the plasmons peak of high intensity and well resolved. But the peaks due to interband transitions near the elastic peak are barely visible. They are less resolved because the plasmons have an influence on them. But, for low primary energy (Ep=500eV); the peaks due to interband transitions are more resolved in particular for IZO (6%In): T_1(4.4eV); T_2(6.6eV); T_3(9.2eV) because the intensity of plasmon peak decreases. Through the comparison between REELS spectra (recorded at 500eV); the interband transitions are in particular more intense for IZO (6% In). Thus; the indium contribution into the ZnO matrix ensures a structural homogeneity of IZO (6%In) thin film as discussed in the XPS; AES and PL parts.

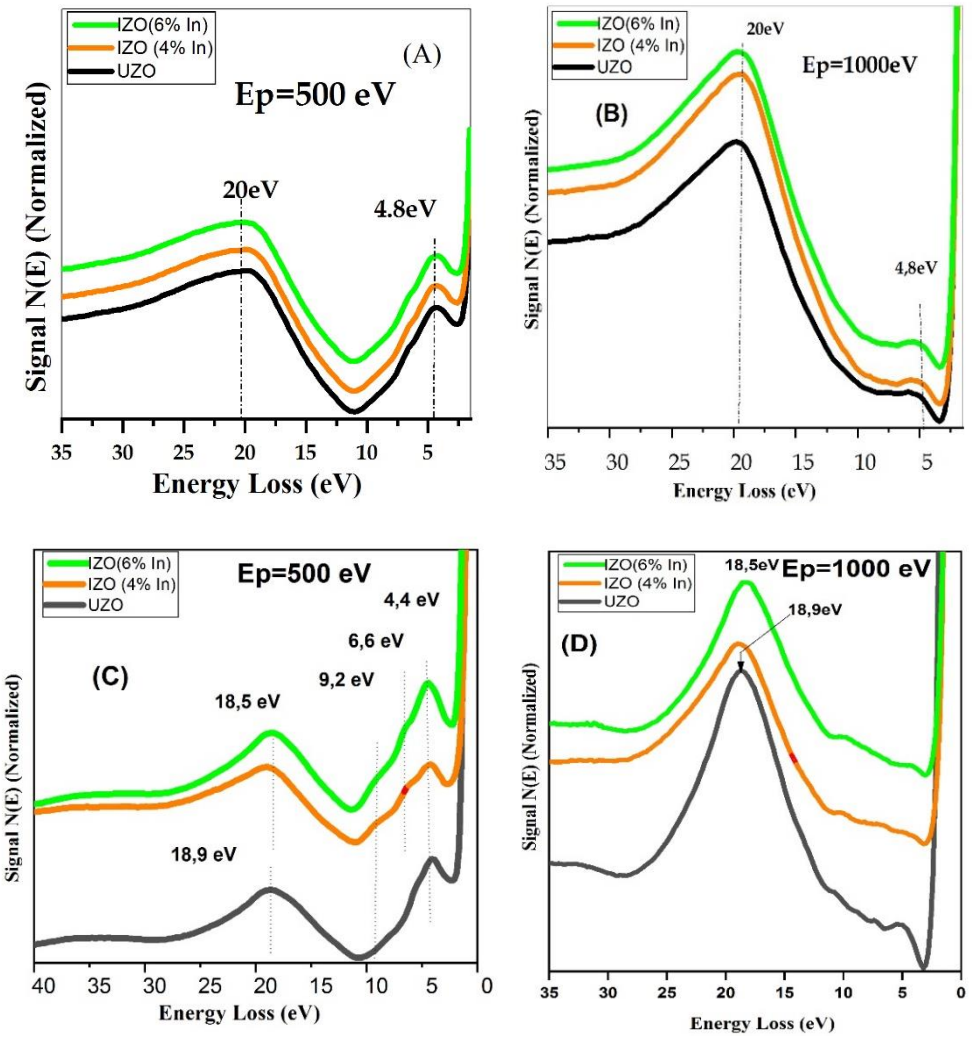


Figure 10. REELS spectra of UZO and IZO at (4% In; 6% In) recorded at different primary energies (Ep=500eV; 1000eV) (A, B) before UHV treatment and (C, D) after UHV treatment

We notice that the interband transitions (T_1:4.4eV occur from (O2p) states); (T_2: 6.6eV and T_3: 9.2eV occur from O2p in hybridation with 3s (O2p-Zn3s) to the conduction band as reported by other authors [53-54].

4. Conclusion

In this work we study the influence of appropriate UHV treatment on Un-doped ZnO (UZO) and In doped ZnO (IZO) (4% In and 6% In) thin films grown on the substrate Si.

The characterization of samples is achieved in ultra-high vacuum (UHV) by the sensitive analysis techniques XPS (X-rays Photoelectron Spectroscopy), AES (Auger Electron Spectroscopy), REELS (Reflection Electron Energy-Loss Spectroscopy) and PL (photoluminescence) for displaying their chemical composition and physical structure. The

analysis techniques XPS and AES show that the checked UHV treatment (argon ion sputtering followed by successive heating until 650°C) allows the convenient incorporation of indium into the ZnO lattice to form chemical species of In-O-Zn type. The UHV treatment is of great interest for inducing a structural homogeneity of thin films IZO (6% In). The recorded REELS spectra confirm this result.

The PL measurements show that the green emission (due to interstitial Oi of UZO) reduces significantly after the incorporation of In into ZnO matrix. The PL measurements also justify that the UHV treatment plays an important role to improve physical structure of IZO (6% In). There is compensation of zinc vacancies (V_{Zn}) by indium atoms to create the electron states (In_{Zn}) and elimination of structural defects due to interstitial zinc (Zni). In this study, we establish a useful complementarity link between the analysis techniques XPS; AES; PL and REELS.

Reference

[1] A. Mang, K. Reimann, Solid state communications, 94.4 (1995): 251-254.

[2] K. Keis, E. Magnusson, H. Lindstrom, S.E. Lindquist, A. Hagfeldt, Solar Energy Mater, Solar Cells 73 (2002) 51–58

[3] J.C. Fan, K. Sreekanth, Z. Xie, S. Chang, K.V. Rao, p-Type *ZnO materials: theory, growth, properties and devices*, Prog. Mater. Sci. 58, 874–985 (2013)

[4] T.K. Gupta, J. Am. Ceram. Soc. 73 (1990) 1817–1840

[5] Z.L. Wang, J.H. Song, Science 312 (2006) 242–246

[6] N. Izyumskaya, A. Tahira, Z. H. Ibupoto, N. Lewinski, V. Avrutin, Ü. Özgür, et al, Review, ECS Journal of Solid State Science and Technology, 6.8 (2017) Q84-Q100

[7] K.M. Sandeep, Shreesha Bhat and S.M. Dharmaprakash, *Structural, optical, and LED characteristics of ZnO and Al doped ZnO thin films*, Journal of Physical and Chemistry of Solids, http://dx.doi.org/10.1016/j.jpcs.2017.01.003

[8] K.Ramamoorthy, K.Kumar, R.Chandramohan, K.Sankaranarayanan, Review on Mater. Sci. Eng., B126 (1) (2006)1–15

[9] G.C. Xie, L. Fang, L.P. Peng, G.B. Liu, H.B. Ruan, F. Wu, C.Y. Kong, *Effect of In-doping on the optical constants of ZnO thin films*, Physics Procedia 32 (2012) 651 – 657

[10] K. Khalid Mahmood, A. Ahmad, S.W. Mehran. Surf. Coating. Technol. 352(2018) 231-237

[11] A. Singh, S. Chaudhary, D. K Pandya, Acta Materialia 111 (2016) 1-9

[12] K. Ellmer, R. Mientus, Thin solid films, 516.14 (2008) 4620-4627

[13] Handbook of Transparent Conductors 2011th Edition, David S. Ginley, Hideo Hosono, David C. Paine, Kindle Edition Springer Science & Business Media (2010)

[14] Flat Panel Display Manufacturing, Jun Souk, Shinji Morozumi, John Wiley & Sons (2018)

[15] K. Keis, E. Magnusson, H. Lindstrom, S.E. Lindquist, A. Hagfeldt, Solar Energy Mater, Solar Cells 73 (2002) 51–58

[16] K. Ramamoorthy, K. Kumar, R. Chandramohan, K. Sankaranarayanan, Materials Science and Engineering, B 126.1 (2006) 1-15

[17] D. Kim, I .Yun, H. Kim, Appl. Phys, 10 (2010) 459–462

[18] M. Shaheera, K.G. Girija, Manmeet Kaur, V.Geetha, A.K. Debnath, R.K. Vatsa, K. P. Muthe, S.C. Gadkari, Optical Materials 101 (2020) 109723.

[19] A. P. Rambu, D. Sirbu, A.V. Sandu, G. Prodan, V. Nica, Bull Mater.Sci. 36 (2013) 231–237

[20] C., Falcony, M.A. Aguilar-Frutis, M. García-Hipólito, *Spray Pyrolysis Technique; High-K Dielectric Films and Luminescent Materials: A Review*, Micromachines 2018, *9*, 414.

[21]. J. Wang, Y. Mei, X. Lu, X. Fan, D. Kang, P. Xu, T. Tan, Applied Surface Science, 387 (2016) 779-783

[22]. W. Wang, Q. Feng, K. Jiang, J. Huang, X. Zhang, W. Song, R. Tan. Applied Surface Science, 257.9 (2011) 3884-3887.

[23] L. J. Sun, D. K. He, X.Q. Xu, Z. Zhong, X.P Wu, B.X. Lin, Z.X. Fu. Chinese Physics Letters, 27, 12 (2010) 126802

[24] J. S. Meena, M.C. Chu, Y.C. Chang, H.C. You, R. Singh, P.T. Liu, et al,. Journal of Materials Chemistry C, 1, 40 (2013) 6613-6622

[25] M. Caglar, S. Ilican, Y. Caglar, *Preparation and characterization of ZnO thin films deposited by sol-gel spin coating method*, Journal of Optoelectronics and Advanced Materials Vol. 10, No. 10, October 2008, p. 2578 – 2583.

[26] M. N. Jung, E. S. Lee, T. I. Jeon, et al., Journal of alloys and compounds, 481,1-2 (2009) 649-653

[27] M. Jacquemin, M. J. Genet, E. M. Gaigneaux, D. P. Debecker, Chem Phys Chem, 14, 15 (2013) 3618-3626

[28] M. Guezzoul, M. Bouslama, A.Ouerdane, et al., *Chemical, morphological and optical properties of undoped and Cu-doped ZnO thin films submitted to UHV treatment*, Applied Surface Science (2020) 146302.

[29] Sirshendu Ghosh, Manas Saha and S. K. De, *Tunable surface plasmon resonance and enhanced electrical conductivity of In doped ZnO colloidal nanocrystals*, Nanoscale,

https://doi10.1039/C3NR05608B

[30] Z. Zhu, B. Li, J. Wen, Z. Chen, Z. Chen, et al., *Indium-doped ZnO horizontal nanorods for high on-current field effect transistors*, RSC advances, 7.87 (2017) 54928-54933

[31] Khalid Mahmood, Seung Bin Park and Hyung Jin Sung Yu, *Enhanced photoluminescence, Raman spectra and field-emission behavior of indium-doped ZnO nanostructures,* J. Mater. Chem. C, 2013,1, 3138-3149.

[32] Arpan Kumar Nayak, Seungwon Lee, Young ku Sohnand Debabrata Pradhan, Nanotechnology, 26 (2015) 485601

[33] Crist, P. D. B. V. Handbook of The Elements and Native Oxides (XPS International, Inc.1999), *Vols. 1*

[34] Mahmoud Bedrouni, Bachir Kharroubi, Abdellah Ouerdane, M'hammed Bouslama, M'hamed Guezzoul, Yves Caudano, Kada Belmokhtar Bensassi, Mohammed Bousmaha, Mohamed Amine Bezzerrouk, Azzeddine Mokadem and Mahfoud Abdelkrim, *Effect of indium incorporation, stimulated by UHV treatment, on the chemical, optical and electronic properties of ZnO thin film*, Optical Materials, https://doi.org/10.1016/j.optmat.2020.110560

[35] J.F. Moulder, W.F. Stickle, P.E. Sobol, K.D. Bomben, *Handbook of X-ray Photoelectron Spectroscopy*, Physical Electronics Division, Perkin-Elmer Corporation (1992)

[36] A. Teke, Ü. Özgür, S. Doğan, X. Gu, H. Morkoç, B. Nemeth, J. Nause, and H. O. Everitt, *Excitonic fine structure and recombination dynamics in single-crystalline ZnO*, Physical Review B,70, 19 (2004) 195207.

[37] K. Hamaida, M. Bouslama, M. Ghaffour, F. Besahraoui, et al., *Growth of In2O3 on In Metal and on InSb by the Electron Irradiation*, Surface Review and Letters 19.06 (2012) 1250066

[38] S. Vempati, J. Mitra, P. Dawson, Nanoscale research letters, 7.1 (2012) 470.

[39] Ü. Özgür, Y. I. Alivov, C. Liu, A.Teke, M. A. Reshchikov, S. Doğan, H. Morkoç, 25 Journal of Applied Physics, 98, 4 (2005) 11

[40] B. Lin, Z. Fu, Y. Jia, Applied physics letters, 79, 7 (2001) 943-945

[41] K. Vanheusden, W.L. Warren, C.H. Seager, D.R. Tallant, J.A. Voigt, B.E. Gnade, J. Appl. Phys. 79 (1996) 7983–7990

[42] B. El Filali, J.A. Jaramillo Gomez, T.V. Torchynska, J.L. Casas Espinola, L. Shcherbyna, *Band-edge emission, defects, morphology and structure of in-doped ZnO nanocrystal films*, Optical Materials 89 (2019) 322–328

[43] H. Zeng, G. Duan, Y. Li, S. Yang, X. Xu, W. Cai, Adv. Funct. Mater. 20 (2010) 561–572.

[44] F. Kayaci, S. Vempati, I. Donmez, N. Biyikli, T. Uyar, Nanoscale 6 (2014)

10224–10234.

[45] F. K. Shan, B. I. Kim, G. X. Liu, Z. F. Liu, J. Y. Sohn et al. J. Appl. Phys. 95, 4772 (2004)

[46] F. Stavale, N. Nilius, H. J. Freund. The Journal of Physical Chemistry Letters (2013) 4, 22, 3972-3976

[47] Y. Xu, B. Bo, X. Gao, Z. Qiao, Crystals 9, 5 (2019) 236.

[48] A. B. Djurišić, A. M. C. Ng, X. Y. Chen. Progress in quantum electronics, 34, 4 (2010) 191-259.

[49] H. Zeng, G. Duan, Y. Li, S. Yang, X. Xu, W. Cai, *Blue luminescence of ZnO nanoparticles based on non-equilibrium processes: defect origins and emission controls*, Funct. Mater. 20 (2010) 561 –572

[50] P. H. Carey, F. Ren, D. C. Hays, B. Gila, S. J. Pearton, S. Jang, A. Kuramata, Applied Surface Science, 422 (2017) 179-183.

[51] J. Wang, Q. Li, R. F. Egerton, *Probing the electronic structure of ZnO nanowires by valence electron energy loss spectroscopy*, Micron 38, 4 (2007) 346-353.

[52] A.M. Konovalov, Yu.M. Krynko, Yu.S. Musatenko, M.G. Nakhodkin, Journal of Electron Spectroscopy and Related Phenomena 133 (2003) 27–37

[53] Z. H. Zhang, X. Y. Qi, J. K. Jian, X. F. Duan. Micron, 37, 3 (2006) 229233

[54] E. Fazio, A. M. Mezzasalma, G. Mondio, T. Serafino, F. Barreca, F. Caridi, Applied Surface Science, 257, 6 (2011) 2298-2302.